Neurotoxicology and Teratology 34 (2012) 72–82

Contents lists available at SciVerse ScienceDirect

Neurotoxicology and Teratology

journal homepage: www.elsevier.com/locate/neutera

Trimethyltin-induced neurotoxicity: Gene expression pathway analysis, q-RT-PCR and immunoblotting reveal early effects associated with hippocampal damage and gliosis

A.R. Little *, D.B. Miller, S. Li, M.L. Kashon, J.P. O'Callaghan

Molecular Neurotoxicology Laboratory, Health Effects Research Laboratory, Centers for Disease Control and Prevention-NIOSH, 1095 Willowdale Road, Morgantown, WV 26505, United States

ARTICLE INFO

Article history:
Received 6 April 2011
Received in revised form 19 August 2011
Accepted 14 September 2011
Available online 12 November 2011

Keywords:
Neurotoxicity
Trimethyltin
Neuroinflammation
Ubiquitin–proteosome
Microarray
Neurodegeneration

ABSTRACT

Damage to the CNS results in a complex series of molecular and cellular changes involving the affected targets and the ensuing glial reaction. The initial gene expression events that underlie these cellular responses may serve as early biomarkers of neurotoxicity. Here, we examined gene expression profiles during the initial phase of hippocampal damage resulting from systemic exposure of rats to the organometallic neurotoxicant, trimethyltin (TMT, 8.0 mg/kg, i.p.). Using TMT as a neurodegeneration tool confers several advantages for evaluating molecular events associated with neural damage: 1) regional and cellular targets and time course of damage are known, 2) the blood–brain barrier is not compromised, which limits the contribution of blood-borne factors, e.g. immune, to neural injury responses and 3) known protein and mRNA signatures of TMT-induced neurotoxicity can be used as positive controls to validate novel expression events associated with exposure to this neurotoxicant. Using Affymetrix Gene Chip® to assess gene expression after TMT, combined with Ingenuity Pathway Analysis®, we observed changes consistent for genes known to be affected in hippocampus, while corresponding changes were not detected in cerebellum, a non-target region. In agreement with previous observations, limited changes in expression of inflammation-related genes were observed. Correlated expression profiles were found after exposure to TMT, including changes in gene ontologies associated with neurological disease, cellular assembly and maintenance, as well as signaling pathways associated with cellular stress, energy metabolism and glial activation. Selected gene changes were confirmed from each category by q-RT-PCR and immunoblot analysis. The canonical relationships identified implicate molecular pathways and processes relevant to detection of early stages of hippocampal damage in the TMT model. These observations provide new insight into early events associated with neuronal degeneration and associated glial activation that may serve as the basis for discovery and development of biomarkers of neurotoxicity.

1. Introduction

Toxic insults of the CNS can alter the expression of a variety of genes and proteins. These effects can vary significantly from one neurotoxic exposure to another because the molecular composition of the CNS differs markedly with respect to brain region, the cell types within a given region or even with respect to a specific subcellular element. Indeed, this innate molecular complexity (Heiman et al., 2008) likely serves as the basis for the regional, cellular and subcellular vulnerability to a specific neurotoxic exposure (O'Callaghan and Sriram, 2005). It also serves as an impediment to detecting, much less predicting, the neurotoxic effects of diverse classes of chemicals and chemical mixtures. While our knowledge of molecular changes associated with exposure to a specific neurotoxic agent might be quite extensive, our knowledge of molecular alterations common to all types of neurotoxic exposures remains in its infancy. To address this problem, we have administered known neurotoxic agents that affect different brain regions and the cellular and subcellular constituents in these regions, as a means of discovering and validating a panel of neuronal and glial biomarkers of neurotoxicity (O'Callaghan, 1988, 1993; O'Callaghan and Miller, 1993; O'Callaghan et al., 1995; O'Callaghan and Sriram, 2005). A number of

Abbreviations: BSA, bovine serum albumin; CCL2, chemokine (C–C motif) ligand 2; CDK, cyclin-dependent kinase; ELISA, enzyme-linked immunosorbent assay; ERK, extracellular signal regulated kinase; ESTs, expressed sequence tags; GR, glucocorticoid receptor; GC-RMA, gene chip robust microarray analysis; GFAP, glial fibrillary acidic protein; GSK-3, glycogen synthase kinase-3; HSP, heat shock protein; IL, interleukin; IPA, Ingenuity Pathway Analysis®; LAMP, lysosomal associated membrane protease; MAP, microtubule associated protein; MHC, major histocompatibility complex; q-RT-PCR, quantitative reverse transcriptase polymerase chain reaction; PBDRc, peripheral benzodiazepine receptor; PBS-T, phosphate buffered saline-tween; PS, presenilin; SNAP, synaptosomal associated protein; STAT, signal transducer and activator of transcription; TMT, trimethyltin; TNF, tumor necrosis factor; UCE, uncoupling enzyme.

* Corresponding author. Tel.: +1 304 285 6079; fax: +1 304 285 6220.
E-mail address: jdo5@cdc.gov (A.R. Little).

0892-0362/$ – see front matter © 2011 Published by Elsevier Inc.
doi:10.1016/j.ntt.2011.09.012

neuronal biomarkers of neurotoxicity, some generally distributed and others linked to the affected cell type, have emerged from these investigations. More importantly, the results of these studies have shown that the glial reaction to injury (i.e. gliosis, reactive gliosis) represents a dominant and homotypic response to diverse neurotoxic insults. These latter observations suggest, at least with respect to the induction of gliosis, that a common set of injury-induced changes underlies CNS responses to diverse neurotoxic agents. Nevertheless, what has not evolved from these studies is the identification of the gene or protein changes common to the diverse targets of neurotoxic insults. Efforts to verify toxicant-induced alterations in groups of genes/proteins linked to effectors of disease and injury processes, for example, those associated with inflammatory reactions (Faulkner et al., 2004; Little et al., 2002), have not been borne out experimentally. Thus, identification of molecular alterations associated with diverse types of neurotoxic exposures remains a challenge to the development of widely applicable biomarkers of neurotoxicity, biomarkers that are needed to screen new and existing chemicals for neurotoxic effects. Indeed, implementation of proposed high-throughput screens for toxicity (Hartung, 2009) will rely on examination of toxicity pathways. At least with respect to neurotoxicity, such pathways need to be identified and validated before any broadly applicable approach to neurotoxicity assessment can be introduced.

To date, most biomarkers of neurotoxicity have been established on the basis of a protein-by-protein or a gene-by-gene analysis of the neurotoxic effects of individual compounds. Given the difficulties in establishing a common molecular basis of neurotoxicity using this approach, implementing methodology designed to survey global changes in gene expression, and subject these finding to pathway analysis, offers the potential to reveal patterns of gene and protein alterations common to diverse neurotoxic insults. Here we report the results of a genomic scale assessment of gene expression changes associated with the earliest stages of neuronal injury caused by the known neurotoxicant, TMT. As a neuronal injury model to be surveyed by gene-array analysis, TMT has several advantages. The cellular targets of TMT in the rat brain, the time course of neuronal damage and the time course of glial activation are known and have been quantified (Balaban et al., 1988; Brock and O'Callaghan, 1987; Chang and Dyer, 1983; Little et al., 2002; McCann et al., 1996; Whittington et al., 1989). The blood brain barrier remains intact after exposure to TMT, therefore, the contribution of blood-borne factors to the observed effects is obviated (Little et al., 2002). Finally, a number of protein and mRNA markers of TMT-induced neurotoxicity in the rat have been established (e.g. Brock and O'Callaghan, 1987; Little et al., 2002) and these can be used as internal positive controls for the results of gene array profiling. Using the Affymetrix Gene Chip® microarray, and posthoc pathway analysis with the Ingenuity Pathway Analysis® system, we identified alterations in gene expression during the first 5 days after exposure to TMT; many of the observed changes have not previously been reported for this model neurotoxicant. The associated network functions, canonical pathways and biological functions affected by TMT include cellular structure and maintenance, neurological disease, the ubiquitin–proteosome system and cellular energy metabolism. Insights from these observations may provide the basis for understanding the etiology of the earliest molecular changes common to multiple classes of neurotoxic responses.

2. Materials and methods

2.1. Animal dosing and tissue preparation

Male or female Long–Evans rats, six weeks of age, were obtained from Charles River (Portage, MI). Rats were housed singly in plastic tub cages with aspen shred bedding in a temperature- (21 ± 1 °C) and humidity-controlled ($50 \pm 10\%$) colony room maintained on a 12 h light/12 h dark schedule. Rats received intraperitoneal injections of vehicle (0.9% saline) or TMT hydroxide (8 mg/kg body weight as the free base) TMT was obtained from K&K Laboratories, Division of ICN Biomedical, Cleveland, OH. TMT-treated rats and saline controls (for each time point) were sacrificed at 3 or 5 days after treatment for gene expression analysis. Additional groups of rats were dosed for neuropathology and immunoblot analyses; the latter included the addition of a 7-day post-dosing time point. Following sacrifice by decapitation, hippocampus and cerebellum were dissected, free-hand; the left side immediately was frozen in liquid nitrogen (for RNA extraction) and the right side was homogenized by sonification in hot (85–95 °C) 1% SDS for specific and total protein assays. All samples were stored at −75 °C prior to assay. All procedures were performed under protocols approved by the Institutional Animal Care and Use Committee of West Virginia University and the animal colony was certified by the American Association for Accreditation of Laboratory Animal Care.

2.2. Silver degeneration staining

A separate set of rats was administered TMT as described above. At three days post dosing these rats were anesthetized with pentobarbital (200 mg/kg, i.p.; Veterinary Laboratories, Lenexa, KS) and then perfused transcardially with a perfusion wash solution containing 0.8% NaCl (wt./vol.), 0.4% (wt./vol.) dextrose, 0.8% sucrose (wt./vol.), 0.023% (wt./vol.) calcium chloride (anhydrous), 0.034% (wt./vol.) sodium cacodylate (hydrated; Sigma Cat # C 0250) and a perfusion fix solution containing 4.0% (wt./vol.) paraformaldehyde powder, 4.0% sucrose, 1.434% (wt./vol.) sodium cacodylate (hydrated). The brains then were sectioned and subjected to cupric silver degeneration staining using the facilities of Neuroscience Associates (Knoxville, TN). Multiple brains were embedded in a gelatin matrix using Multi-Brain™ technology (Neuroscience Associates, Knoxville, TN), frozen in isopentane (−70 °C), sectioned in the coronal plane at 40 μm on an AO860 sliding microtome, and collected in 4.0% formaldehyde containing 4.2% sodium cacodylate (pH 7.2). Each large section cut from the block was made up of brains from control and TMT-treated groups to insure uniform staining across groups and every eighth section was stained. Thionine (0.05%) was used as a Nissl stain according to the procedure of Vogt (1968). Amino Cupric Silver Staining was performed according to the method of de Olmos et al. (1994).

2.3. RNA isolation and reverse transcription assay

Total RNA was isolated using Trizol (Invitrogen, Carlsbad, CA). Samples were reverse-transcribed in duplicate using Superscript™ and oligo dT primers™ (Life Technologies/Gibco BRL, Carlsbad, California) using 1–2 μg of total RNA according to the manufacturer's protocol.

2.4. Gene Chip® analysis

Initially, an analysis of TMT-induced changes in gene expression on post-dosing day 5 was obtained using the Affymetrix U34A Gene Chip® (Affymetrix Corporation, Santa Clara, CA). Samples from saline- or TMT-treated hippocampus and cerebellum (as a negative control) were analyzed by pooling samples from 5 rats for each brain area per chip. The successful outcome of these experiments, combined with the availability of a newer Gene Chip® containing 16,000 genes/ESTs, prompted us to use this chip (A230) to obtain data for samples prepared 3 days after exposure to TMT or saline vehicle. In these latter experiments, one chip per rat per brain area was used with a total of 4 animals for each treatment group. Briefly, for both chips, total RNA was isolated from brains of control and TMT-treated rats and purified by phenol/chloroform extraction. Purified RNA (20 μg) was used for preparation of cDNA with the

Superscript Choice System (Invitrogen, Carlsbad, CA). After ammonium acetate extraction and ethanol precipitation, the cDNA was used as a template to produce biotinylated cRNA transcript by in vitro transcription (Enzo, Farmingdale, NY). This cRNA was purified by an ammonium acetate extraction and ethanol precipitation, fragmented with heat and Mg^{2+}, and hybridized to the rat U34A or 230A arrays in the Affymetrix Hybridizaton oven 320. Subsequent washing and staining of the arrays were performed using the Gene Chip Fluidics station protocol Euk-GE-WS2 and scanned using the Affymetrix scanner (Hewlett-Packard, Houston, TX).

2.5. Molecular pathway analysis

To understand how the genes identified by inferential statistics are related, Ingenuity Pathway Analysis (IPA) software (Ingenuity® Systems, Inc., Redwood City, CA) (www.ingenuity.com) was used to identify biologically relevant networks, biological functions and canonical pathways affected early after TMT exposure. The whole data set generated from the A230 Gene Chip containing gene identifiers and their corresponding expression values were uploaded into the application and a core analysis was conducted to identify networks of genes as well as biological functions affected by the treatment. A fold change cutoff of 1.4 was used to identify the genes whose expression was affected by the TMT treatment. The identified genes, known as Network Eligible genes or "focus" genes, were overlaid onto a global molecular network developed from information contained in Ingenuity's Knowledge Base. These "focus genes" were used to query the database for interactions between focus genes and all other gene objects stored in the base to construct biological networks with a statistical score determined for each network. This score indicates the probability of the focus genes being linked in a network due to random chance. In these networks the differentially regulated genes can be related using previously known associations between genes but are independent of established canonical pathways.

The data set was subjected to canonical pathways analysis to identify the pathways from the Ingenuity Pathways Analysis library of canonical pathways that were most significant to the data set. A canonical pathway contains the genes related to a particular process such as oxidative phosphorylation or signaling through a given pathway (e.g. ERK). The canonical pathways contained in the Ingenuity database are developed by a comprehensive assessment of the extant literature and are updated on a regular basis as new data emerge. Our analyses were current to November 1, 2010. Only genes from the data set that met the cut-off expression value of 1.4 or greater and were associated with one of the canonical pathways found in Ingenuity's Knowledge Base were included in the analysis. The significance of the association between the data set and the identified canonical pathways was measured in 2 ways: 1) a ratio of the number of molecules from the data set that map to the pathway divided by the total number of molecules in the knowledge base that map to that canonical pathway and 2) Fisher's exact test to calculate a p-value determining the probability that the association between the genes in the data set and the identified canonical pathway is due to chance alone.

The Biological Functional Analysis component of the IPA software was also used to evaluate the uploaded database to identify the biological functions and/or diseases that were most significant to the genes in the data set. This analysis provides information on the biological functions or diseases that were impacted by TMT treatment. Genes in the data set that met the criterion of a 1.4 fold expression cut-off and were associated with biological functions and/or diseases in the Ingenuity knowledge base were included in the analysis. A right-tailed Fischer's exact test was used to calculate a p-value determining the probability that each function or disease assigned to the data set was due to chance alone.

2.6. Real-time PCR

Candidate genes from the results of the Gene Chip® and IPA analysis were assayed by real-time PCR (q-RT-PCR) using Taq-man technology (PE Biosystems, Carlsbad, CA) as previously described (Little et al., 2002). Briefly, fully amplified (40 cycles) PCR products of each cDNA of interest were quantified using 260/280 ratios on a Beckman DU650 spectrophotometer and were serially diluted in 10-fold increments. These samples were run on the same plate as samples used for a standard curve. Standard curves were highly linear over 7–9 orders of magnitude with correlation coefficients typically at or above 0.995. Samples from each time-point were run together (controls and TMT on the same plate), as was the 28S or S29 housekeeping gene in separate wells. PCR reactions were conducted with primer concentrations of 300 nM. A 2× Master Mix (PE Biosystems, Carlsbad, CA) diluted in water was used to bring the final reaction volume to 50 µl. Primers were made using Primer Express® (Applied Biosystems, Carlsbad, CA) and Amplify software based on accession numbers of sequences used on the Affymetrix chip (Table 1).

2.7. Total protein assay

Total protein concentration of the homogenates was assayed by the method of Smith et al. (1985). BSA was used as a standard.

Table 1
Primers used.

Gene name and ID	Size	Primer sequence	Source
Tau 5′ NM_017212	74	ACACATCTCCACGGCACCTCAG	Developed in house (DIH)
Tau 3′		CAAGCTGTGGAGAGTCCACCA	
PS1 5′ NM_019163	79	ATGATGGTGGCTTCAGTGAGG	DIH
PS1 3′		TCTTGCCAAGCCAATCCC	
PS2 5′ NM_031087	86	AGACTGGAGCACGACGCTGGCCTGCTT	DIH
PS2 3′		TTCTTGAACACGGCGAGCAGCAGGA	
UCE-E2D3 5′ NM_031237	69	TTTGGCCGGACCTTTGAG	DIH
UCE-E2D3 3′		GCGCCATAGTCTGTGCTTTTC	
UCE 5′ AA799453	62	TTGCCCCCTCATAAGCAGC	DIH
UCE 3′		TCTTGCCAAGCCAATCCC	
GR 5′ NM_012576.1	72	GCATCTTCAGAACAGCAAAATCG	DIH
GR 3′		TGGGATACAATTTCACACTGCC	
STAT5a 5′ NM_017064.1	78	GTGTGCCCTCAGGCTCACTAC	DIH
STAT5a 3′		GGTCAAATTCACCATCTTGGTCA	
Ccl2 5′ NM_031530	395	TGCTGCTACTCATTCACTGGCAA	McTigue et al. (1998)
Ccl2 3′		CTGCTGCTGGTGATTCTCTTGT	
GFAP 5′	250	GCTAGCTACATCGAGAAGGTC	Hauss-Wegrzyniak et al. (1998)
GFAP 3′		TCCAGCCTCAGGTTGGTTTCA	
CCR2		Proprietary	Applied Biosystems
CCR5		Proprietary	Applied Biosystems
TNF-α		Proprietary	Applied Biosystems
IL-1α		Proprietary	Applied Biosystems
IL-1β		Proprietary	Applied Biosystems
LAMP1		Proprietary	Applied Biosystems
SNAP25		Proprietary	Applied Biosystems
S29 5′ BC058150	265	CGCTCTTGCCGCGTCT	DIH
S29 3′		CACATGTTCAGCCCGTATTT	

2.8. Immunoblot analysis

Changes in expression of selected proteins, chosen on the basis of changes observed from the Gene Chip® and qPCR analysis, were analyzed by immunoblotting. Aliquots of brain homogenate were diluted in sample buffer, boiled and loaded on 10% SDS-polyacrylamide gels (Laemmli, 1970). Proteins were electrophoretically resolved and transferred to 0.1 μm nitrocellulose membranes (Tobin et al., 1979). Subsequent steps were performed at room temperature. Membranes were blocked for 1 h in 5% non-fat dry milk prepared in PBS-T, washed (1×15 min; 2×5 min) with PBS-T and incubated with the following antibodies at 1:500 for 2 h: PS2 (cs-2192) (Cell Signaling Technology, Beverly, MA), SNAP25 (ab 18002) (Abcam, Cambridge, MA) and LAMP1 (9234) Gene Tex, Irvine, TX). Blots then were washed with PBS-T (1×15 min; 2×5 min) and incubated with anti-rabbit IgG-HRP conjugate (1:2500) for 1 h. Except for SNAP25 and LAMP1, membranes were washed in PBS-T (1×15 min; 4×5 min) and detection was achieved using a chemiluminescent substrate Amersham ECL (Piscataway, NJ, USA) on X-ray film (Fuji Medical Systems, Stamford, CT). Films were exposed for 10 s to 3 min depending on signal intensity. Films were scanned using a Molecular Dynamics PDSI scanner and software (Version 4.0) and quantified using Imagequant (Version 5.2) software. For SNAP25 and LAMP1, membranes were washed in PBS-T (1×15 min; 4×5 min) and detection and quantification was achieved using Odyssey version 3.0 and scanned by LiCor (Odyssey 9120, Lincoln, NB). An approximate linear relationship between the total protein load per gel lane and the signal obtained was established for each protein as previously described (O'Callaghan et al., 1999).

2.9. Statistical analyses

Microarray data were analyzed using R statistical software and packages from Bioconductor (Gentleman et al., 2004). Initial intensity values in .cel files were subjected to background correction, normalization and probe set summarization using GC-RMA method in the "gcrma" package. Establishing the presence or absence of genes was performed using the Wilcoxon signed rank-based test using the "affy" package. Undetected genes were removed from further analysis. Group comparison p-values were obtained by using a *t*-test using "limma" package with empirical Bayes variance estimation. The control for false discovery rate was implemented by the Benjamini and Hochberg (1995) approach and expression summary data were formatted for input in to Ingenuity Pathway Analysis Software (see Molecular Pathway Analysis above). PCR and immunoblots analyses were performed using JMP (version 6.0.3) statistical analysis software. The test of significance for individual variables was performed using one-way analysis of variance (ANOVA) followed by posthoc analysis using Student–Newman–Keuls test.

3. Results

3.1. Onset of trimethyltin-induced neuronal degeneration in hippocampus

Nissl stains reveal some evidence for degeneration of hippocampal dentate granule cells as early as three days after administration of TMT to the rat (Chang and Dyer, 1983; Whittington et al., 1989). In contrast, sensitive silver degeneration stains have been reported to reveal some damage to both pyramidal and dentate granule cells as early as post-dosing day 2 (Balaban et al., 1988), observations consistent with evidence of microglial activation at the same post-dosing time point (Little et al., 2002; McCann et al., 1996) as well as the ensuing astrogliosis by no later than post-dosing day 5 (Brock and O'Callaghan, 1987; Little et al., 2002). The cupric silver degeneration staining shown in Fig. 1 confirms extensive TMT-induced-degeneration of pyramidal and dentate neurons throughout the dorsal hippocampus by post-dosing day 3, findings in agreement with those reported by Balaban et al. (1988) using a slightly different variant of the cupric silver stain. Nissl staining of alternate sections did not reveal overt changes at the same time point (data not shown). Together, these data serve as the basis for our choice of post-dosing day 3 as the earliest time point to survey for gene-expression changes associated with the onset of TMT-induced neuronal degeneration in the hippocampus. The lack of evidence for damage to cerebellum at the same time point, as determined by a variety of procedures (e.g.

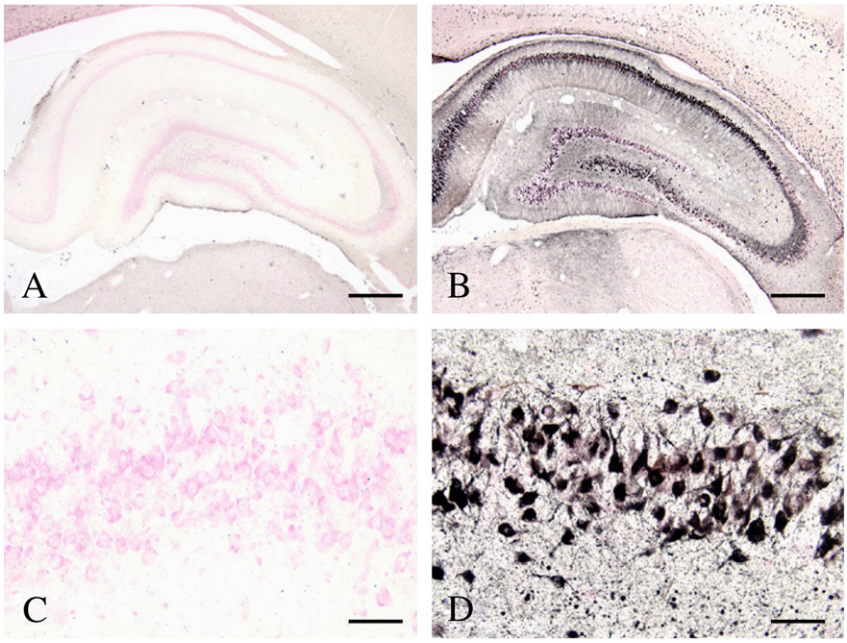

Fig. 1. Silver degeneration staining reveals extensive hippocampal neuronal damage at 3 days after administration of TMT (8.0 mg/kg, i.p.) (B and D). Amino cupric silver degeneration staining shows argyrophic neurons throughout the pyramidal cell line and the dentate gyrus after TMT (B). Higher magnification shows argyrophilic pyramidal neurons in CA3 region after TMT (D). Corresponding saline controls are shown in A and C. Neutral red is used as a counter stain. Scale bar = 500 and 100 μm for A–B and C–D, respectively.

see Balaban et al., 1988; Chang and Dyer, 1983), dictated our use of this region as a negative control for changes observed in samples from hippocampus.

3.2. Gene Chip® analysis verifies gene expression changes associated with TMT-induced neuronal degeneration and gliosis and reveals novel gene-expression patterns during the earliest stage of hippocampal neurodegeneration

To determine if gene expression changes known to be associated with the earliest phase of hippocampal degeneration due to TMT could be detected by oligonucleotide array analysis, we used the Affymetrix U34A Gene Chip® to interrogate approximately 8000 genes and ESTs. Initially, rats were sacrificed at post-dosing day 5, a positive control time point, i.e. one coinciding with the earliest evidence for enhanced expression of multiple glial proteins resulting from the onset of TMT-induced neuronal damage (e.g. see Brock and O'Callaghan, 1987; Little et al., 2002). Samples prepared from cerebellum served as negative controls. A total of 228 genes showed more than a 1.3-fold change in expression (up or down) in hippocampus after TMT, in comparison to values obtained from saline controls (data not shown). Notably, Gene Chip® analysis verified increased expression of genes known to serve as markers for injury-induced activation of microglia (CCL2, MHC-I and MHCII) and astroglia (GFAP, vimentin, glutamine synthetase and PBDRc) (Fig. 2), findings that confirm known microglial and astroglial responses to TMT-induced hippocampal damage observed in this and other laboratories (Andersson et al., 1994; Banati et al., 1997; Bo et al., 1994; Brock and O'Callaghan, 1987; Cammer et al., 1989; Condorelli et al., 1990; Finsen et al., 1993; Guilarte et al., 1995; Kuhlmann and Guilarte, 1997, 1999; Little et al., 2002; Mikucki and Oblinger, 1991; Shaw et al., 1994; Stringer, 1996; Xu and Ling, 1994). Although detected, none of the more than 20 interleukin, interferon, or TNF super family genes on the U34A array was induced by TMT at day 5 (data not shown). These latter findings are consistent with our previously reported negative results for IL-1β, TNF-α, and IL-6, using q-RT-PCR analysis (Little et al., 2002). Likewise, expression of the bulk of cerebellar genes remained unchanged as a function of TMT exposure; the known expression pattern for glial genes observed for hippocampus (Fig. 2) did not emerge in the cerebellum (data not shown). In aggregate, the data obtained for gene expression on post-dosing day 5 were highly consistent with known changes in glial gene expression that follow the onset of neurodegeneration due to TMT. This successful outcome combined with the knowledge that neuronal damage due to TMT was ongoing prior to post-dosing day 5 (see Fig. 1) prompted us to evaluate gene-expression patterns at post-dosing day 3. For this purpose we used the A230 Gene Chip® to expand analysis to 16,000 genes and ESTs. A total of 207 genes exhibited more than 1.4 fold change in expression (up or down) in hippocampus after TMT, in comparison to values obtained from saline controls. Representative examples of these data organized by gene class are presented in Table 2. The fold changes in these genes were not large; these observations were consistent with sampling a time point at the very earliest stage of TMT-induced neurodegeneration. This fact, coupled with the low number of Gene Chips® used (N = 4), probably contributed to the lack of statistical significance among all the gene-expression changes observed as a function of exposure to TMT. Indeed, our findings with the Gene Chips® speak to the value of performing a priori power analyses for future experiments to inform experimental design and hypothesis generation (Seo et al., 2006). Nevertheless, these data provided a qualitative index of early expression changes associated with the onset of TMT-induced neurodegeneration that, in conjunction with Ingenuity® Pathway Analysis, were used to inform subsequent q-RT-PCR analyses. Consistent with our previous findings based on q-RT-PCR (Little et al., 2002), qualitative changes in genes associated with inflammation were notably absent from day 3 and day 5 data (data not shown), suggesting that inflammatory processes were not in play during the early stages of neuronal degeneration caused by TMT.

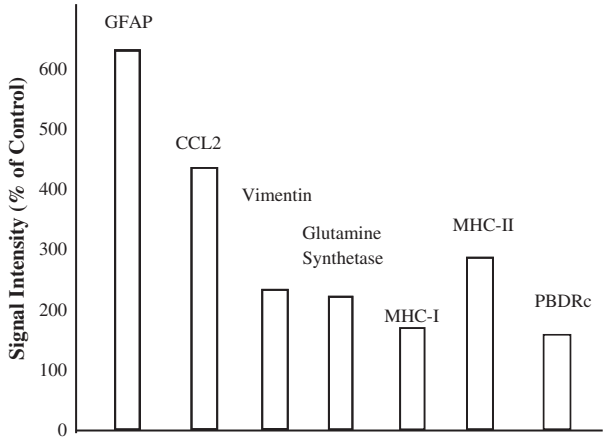

Fig. 2. Induction of astroglial- and microglial-associated genes at 5 days after administration of TMT (8.0 mg/kg, i.p.). Data are based on microarray results from hippocampal tissue pooled from 5 saline- and 5 TMT-treated rats (i.e., N = 1 per treatment and brain area) and are expressed as a percent of saline control data.

3.3. Ingenuity® Pathway Analysis reveals relationships among networks and molecules related to neurological disease, cellular assembly and maintenance, and mitochondrial function

Using a fold change cutoff of 1.4, a total of 229 focus genes were identified whose expression was affected early after TMT treatment. Using these focus genes to interrogate the Ingenuity Knowledge Base, 14 networks were constructed and found to be significant with scores ranging from 8 to 50, where the Fisher's exact test indicates any score over 2 is significant. For simplicity, only the networks with significant scores (8 or above) and those deemed useful for providing insight related to early neurotoxic events associated with exposure to TMT (post-dosing day 3) are presented. The networks are presented as graphical displays where the genes appear as nodes and the molecular relationships between genes are represented by lines. The network titles refer to the primary functions of the gene pathways identified as the pathway analysis seeks to discern the connections between the genes affected by the TMT treatment through the knowledge contained in the IPA database. As such the analysis is not dependent on the study design and is not hypothesis driven. Consequently, the networks identified as being affected by TMT treatment are based on the known functions and interconnectivity of the affected genes derived from the literature and placed in the IPA knowledge base.

The genes contributing to the highest scoring network in the hippocampus at 3 days post TMT exposure were those involved in cellular assembly and organization, cellular function and maintenance as well as neurological disease (Fig. 3). Of the top 5 network functions affected by TMT, the highly significant scores ranged from 28 to 50 (Table 3). The top network (with a score of 50, see Table 3 and Fig. 3) incorporated 27 focus genes out of the 35 eligible genes. A variety of nodes consisting of genes associated with signaling molecules were significantly down-regulated (green), including inputs to the key proinflammatory transcription factor, NF-kB. Nodes including structural and motor molecules were also decreased whereas cellular distress signaling through HSP90 was increased (red). Additional analysis of the data set using the Canonical Pathway (Table 4) and Biological Functional Analysis (Table 5) components of the IPA software, revealed a number of known processes and biological functions affected by TMT exposure. These analyses in

Table 2
Microarray data at 3 days after TMT.

Gene grouping by function	A230 gene ID	Fold change
Neuronal		
Synaptophysin	NM_012664.1	0.56
Serotonin 5HT-2 receptor gene	NM_021862.1	1.34
GABA-alpha receptor gamma-3 subunit	NM_024370.1	1.50
Proteolipid protein (spastic paraplegia 2)	NM_030990.1	0.49
Amphiphysin	NM_022217.1	1.37
Superiorcervical ganglia, neural specific 10	NM_053440.1	0.58
Neurofilament, light polypeptide	NM_031783.1	0.80
Receptors		
Mitochondrial precursor receptor	D63411.1	1.48
Stromal cell derived factor receptor 1 (Sdfr1)	NM_019380.1	0.56
Somatostatin 28 receptor	NM_133522.1	0.69
Somatostatin sst2B receptor	X98234.1	0.69
Phosphatases, kinases		
Protein tyrosine phosphatase epsilon C	D78610.1	0.60
Calcineurin subunit A alpha	NM_017041.1	0.62
STAT5a	NM_017064.1	1.47
RhoB	NM_022542.1	0.76
Glycogen synthase kinase 3 alpha (Gsk3α)	NM_017344.1	1.33
Myristoylated alanine-rich protein kinase C substrate	BE111706	1.33
Protein tyrosine kinase	NM_013081.1	0.62
Metabolism		
Aromatic L-amino acid decarboxylase	U31884.1	0.24
Myoadenylate deaminase (AMP deaminase)	J02811.1	1.23
Sterol carrier protein 2	M34728.1	0.43
3-Hydroxy-3-methylglutaryl-coenzyme A synthase1	NM_017268.1	0.65
Hypoxanthine-guanine phosporibosyltransferase	M86443.1	0.51
Mitochondrial precursor receptor	D63411.1	1.48
Development/growth factors		
Adducin 3, gamma	AA894279	0.68
TGF-beta 3	NM_013174.1	0.59
Structural		
Kinesin-family protein 1Bp204	AB070355.1	1.70
Opioid-binding protein cell adhesion molecule-like	NM_053848.1	1.29
Neurodegeneration		
Tau	X79321	1.24
Presenilin (PS) 1	NM_019163.1	1.68
Presenilin (PS) 2	NM_031087.1	ND
BM1k MHC class Ib antigen	AJ243973.1	1.58
Stress/chaperone		
Heat shock protein 60	NM_022229.1	0.72
Transcription/translation/degradation		
Arf2, ADP-ribosylation factor 2	BE112160	5.23
Ubiquitin conjugating enzyme (E2D) (E217kB?)	U13177.1	0.69
Ubiquitin conjugating enzyme (UCE)	NM_031138.1	2.77
Ubiquitin conjugating enzyme E2I	NM_013050.1	1.53
Ribosomal protein S2	AA944861	0.71
Ribosomal protein L4	NM_022510.1	1.67
Ribosomal protein S27	BI281702	0.72
Miscellaneous		
Spermatogenesis related protein Gs4	NM_138855.1	0.59
mRNA for 5I2 antigen, clone 5	NM_019301.1	1.88
hnRNP protein	BM384165	0.68
Alpha-actinin-2 associated LIM protein	AF002281.1	1.32
Opioid-binding protein	NM_053848.1	1.32
Golgi vesicular membrane trafficking protein p18	NM_01925	0.26
SMR2	NM_022709.1	0.55
Transforming growth factor beta 1 induced transcript 1	BI279862	1.30
Heterogeneous nuclear ribonucleoprotein K	NM_057141.1	0.68
Pore-forming calcium channel alpha-1B Subunit variant	AF055477.1	1.6
Endothelial type gp91-phox gene	NM_023965.1	0.53
Cytokine-induced neutrophilchemoattractant-2 beta	D21095.1	2.13
Transcription factors/signaling		
Nuclear receptor subfamily 3, group C, member 1 (Nr3c1) Corticosteroid Receptor	NM_012576.1	1.71
PAM COOH-terminal interactor protein 10b	U88156.1	1.32
Sphingomyelin phosphodiesterase 3, neutral	NM_053605.1	1.86
Phospholipase C-beta1	BE097028	0.74
Apoptosis		
Bcl-2 related ovarian death gene product BOD-L	AF065433.1	1.48

conjunction with the results from the network analysis (Table 3) showed highly significant changes in events related to a variety of cell signaling processes, cell morphology and mitochondrial function. Of these three types of changes, signaling and morphology are known components of glial response to injury and mitochondria have long been viewed as potential targets of TMT (Chang et al., 1982; Cook et al., 1984).

Biological Functional Pathway analysis of the TMT database (Table 5) also categorized affected genes into a number of higher level biological entities, including diseases and disorders; molecular and cellular functions as well as physiological system development and function. Each of these higher level categories contains several lower level categories as indicated by the subcategories and their associated p-values. For example, the diseases and disorders category has p-values ranging from 2.01E−09 to 8.66E−04 and contains subsets of all the genes in the category that are relevant to genetic (140 relevant genes) and neurological (111 relevant genes) disorders as well as those considered important in developmental disorders (9 relevant genes). This analysis again highlights the early effects of TMT on processes and functions related to cell morphology and function as well neurological disease.

Table 6 shows the top 10 up-regulated and down-regulated genes in the rat hippocampus following TMT treatment (ranked by the magnitude of fold-change). The top molecular changes included increases in LAMP1, a lysosomal membrane protein, along with an expected increase in the astrocyte protein, GFAP. Among the top three decreases in molecules was SNAP25, a finding suggestive of early loss in synapses, a finding also consistent with the previously observed change in synaptophysin (p38) and synapsin (Brock and O'Callaghan, 1987).

3.4. Selected gene expression analysis by q-RT-PCR

In addition to the top molecules identified by IPA, the top network functions, canonical pathways and biological functions identified by IPA served to direct the selection of specific candidate genes for further analysis. From each of these IPA-directed categories, we selected IPA-identified molecules, as well as genes from the microarray analysis with the greatest changes in expression, to be verified by q-RT-PCR using RNA prepared from a separate set of animals (Fig. 4). Consistent with IPA results, lysosomal and synaptic genes, LAMP1 and SNAP25, showed small but significant increases and decreases, respectively, findings that suggested mitochondria and synaptic terminals were early targets of TMT-induced neurotoxicity. Other mitochondrial signaling genes and intracellular receptor and translocation genes identified or implicated by microarray analysis also were affected. Increases in STAT5a, UBC and GR were dramatic and, while increases in STAT5a and UBC were not statistically significant at 3 days, they were by 5 days post TMT. GR and PS1 increases at day 3 were confirmed by PCR while PS2, β-catenin, and Tau could not be confirmed at day 3 but all were significantly increased by 5 days (Fig. 4).

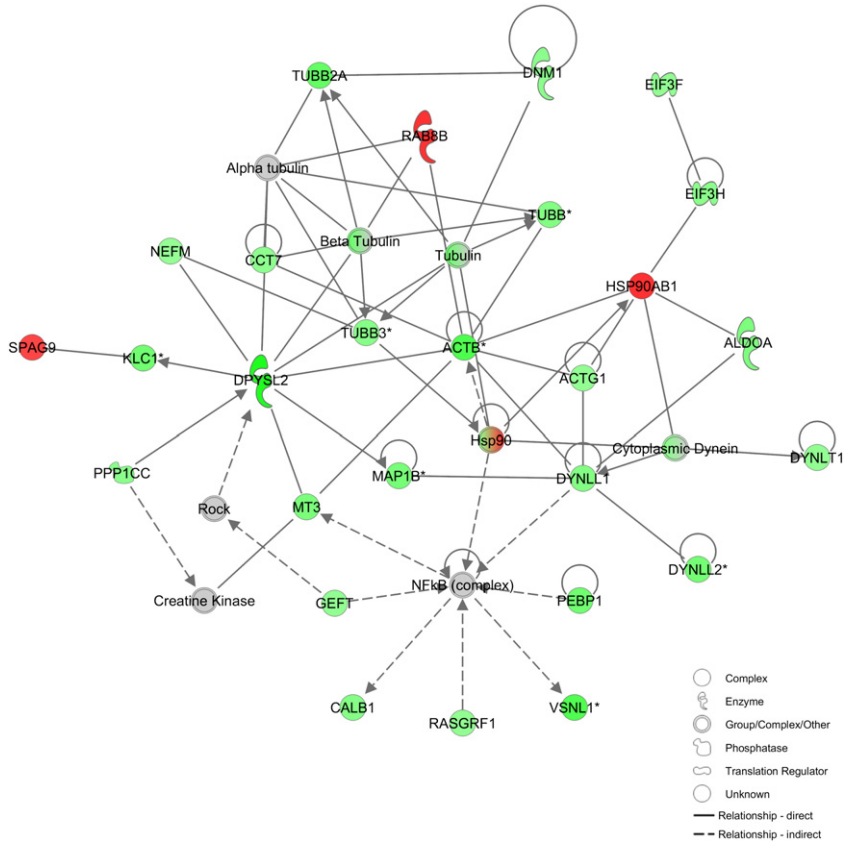

Fig. 3. The top network of differentially expressed focus genes in the rat hippocampus 3 days after administration of TMT (8.0 mg/kg, i.p.) as identified by IPA analysis. Intensity of the red (up-regulated) or green (down-regulated) color shows the level of gene expression. Gray represents a gene found in the TMT data set but one that did not meet the cutoff criteria of 1.4 fold.

3.5. Immunoblot analysis of selected proteins based on q-RT-PCR data

To assess the correlation between gene and protein expression changes resulting from exposure to TMT, immunoblots for proteins implicated by IPA and q-RT-PCR were performed (Fig. 5). For most of the proteins analyzed, post-dosing day 3, 5, and 7 time points were examined. Several of our attempts to extend q-RT-PCR findings to corresponding proteins failed due to a lack of apparent confirmation by immunoblot or a failure to obtain discernable results on immunoblots (data not shown). Nevertheless, several changes suggested by the IPA and q-RT-PCR data were confirmed at the protein level (Fig. 5). At 3 days after TMT treatment, the 23 kD c-terminal fragment of PS2 was increased by nearly 2 fold. SNAP 25 was decreased by day 5, whereas LAMP1 was increased by 7 days post TMT. Overall, these data for selected proteins are consistent with results obtained with the oligonucleotide arrays, IPA and q-RT-PCR, or previously published data, and they are suggestive of the functional significance of the observed changes in gene expression.

Table 3
IPA® associated network functions.

Score	
1 Cellular assembly and organization, cellular function and maintenance, neurological disease	50
2 Cell signaling, cellular function and maintenance, molecular transport	45
3 Post-translational modification, protein folding, genetic disorder	45
4 Cell-to-cell signaling and interaction, nervous system development and function, genetic disorder	39
5 Lipid metabolism, small molecule biochemistry, cell morphology	28

Table 4
IPA® top canonical pathways.

Score	
Oxidative phosphorylation	2.77E−07
14-3-3-mediated Signaling	1.85E−05
ERK5 signaling	3.13E−04
Mitochondrial dysfunction	4.75E−04
Clathrin-mediated endocytosis signaling	5.58E−04

Table 5
IPA® top biological functions.

Name	p-value	# Molecules
Diseases and disorders		
Genetic disorder	2.01E−09–3.86E−02	140
Neurological disease	2.01E−09–4.60E−02	111
Psychological disorders	2.01E−09–3.35E−02	56
Skeletal and muscular disorders	5.91E−09–2.73E−02	79
Developmental disorder	8.66E−04–2.73E−02	9
Molecular and cellular functions		
Cellular assembly and organization	1.63E−04–4.81E−02	53
Cellular function and maintenance	1.63E−04–3.86E−02	21
Protein synthesis	2.34E−04–3.18E−02	34
Cell morphology	3.45E−04–3.86E−02	44
Cell-to-cell signaling and interaction	5.92E−04–4.49E−02	30
Physiological system development and function		
Nervous system development and function	8.44E−06–4.58E−02	69
Tissue development	8.44E−06–3.86E−02	17
Behavior	1.49E−04–2.88E−02	15
Embryonic development	4.04E−03–2.65E−02	9
Organ development	4.04E−03–2.65E−02	12

Table 6
IPA ® top molecules.

Fold change up-regulated	
Molecules	Exp. value
LAMP1	↑2.517
GFAP	↑2.421
HTRC	↑2.405
HSP90AB1	↑1.922
CORO6	↑1.863
RAB8B	↑1.841
IGF2R	↑1.765
MEIS2	↑1.728
RIOK2	↑1.721
MBNL2	↑1.646
Fold change down-regulated	
Molecules	Exp. value
DCAF6	↓−6.540
IDS	↓−4.788
SNAP25	↓−4.301

4. Discussion

We used the known neurotoxicant, TMT, to identify gene expression changes associated with the earliest stages of neurodegeneration and gliosis. Previously, many features of TMT neurotoxicity have been established that provided the basis for choosing this compound as a neural degeneration tool. Multiple, independent, morphological and biochemical indices have established the time-course of TMT-induced damage to the hippocampus and the accompanying microglial and astroglial responses (Brock and O'Callaghan, 1987; Chang and Dyer, 1983; Little et al., 2002; McCann et al., 1996). Sensitive neuronal, microglial and astroglial staining methods show that TMT-induced damage to hippocampal pyramidal and dentate neurons can occur as early as 2–3 days post dosing and that this damage likely is responsible for the rapid activation of microglia and astroglia (Balaban et al., 1988) (Fig. 1). Importantly, the blood brain barrier remains intact, limiting the contribution of blood-borne factors to the initiation or progression of damage and gliosis (Little et al., 2002). Despite the severe neuronal loss that eventually results from exposure to TMT, we found that early gene expression events were restricted to relatively small numbers of transcripts. These were clustered into networks and relationships that may serve to inform our knowledge of mechanisms of neural damage and gliosis that underlie neurotoxic responses to this compound, and perhaps broader classes of neurotoxicants.

We conducted our initial gene-array survey at 5 days post-dosing with TMT to determine if we would capture known expression events related to the neurotoxic effects of this compound. This qualitative survey, not unexpectedly, revealed enhanced expression of numerous glial genes in hippocampus, while these same genes remained unchanged in the cerebellum, a non-target region for TMT. Thus, our use of oligonucleotide microarrays to survey genes expressed just after the onset of TMT-induced hippocampal neurotoxicity was successful in confirming known glial responses to neural damage (Balaban et al., 1988; Brock and O'Callaghan, 1987; Kuhlmann and Guilarte, 1997, 1999; Little et al., 2002; McCann et al., 1996). Because such glial responses are shared across numerous, trauma-disease and chemically-induced insults of the CNS (Eng et al., 2000; Kreutzberg, 1996; Norenberg, 2005; O'Callaghan and Sriram, 2005; Sofroniew, 2005, 2009; Streit, 2005), raised the possibility that gene expression events occurring prior to glial activation may be shared across multiple models of neural damage. Such changes in gene expression, in turn, may serve as the basis for discovering early molecular processes

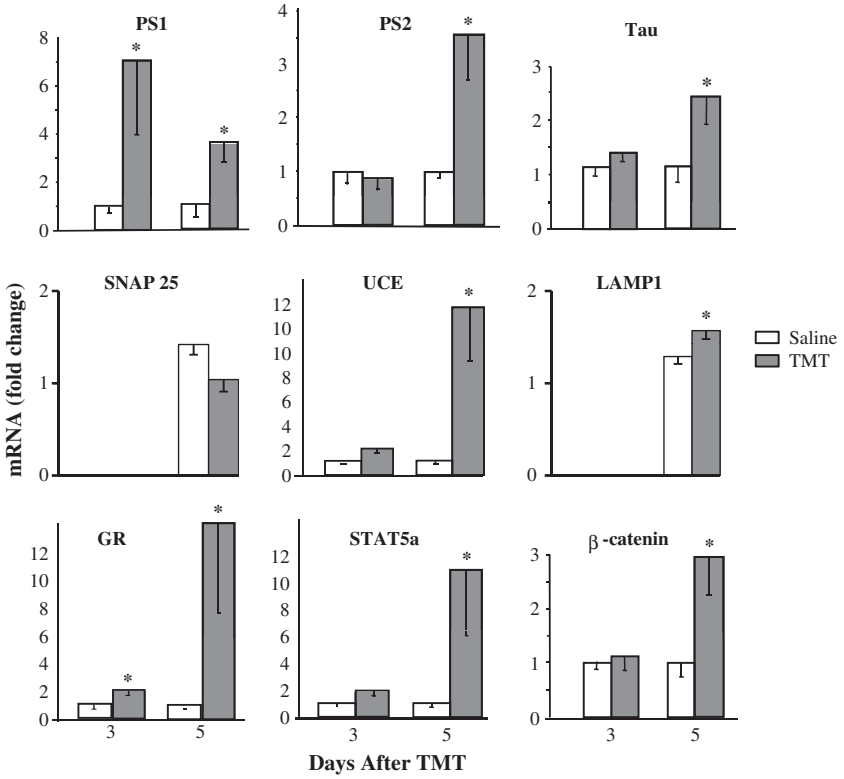

Fig. 4. Changes in gene expression by q-RT-PCR analysis at 3 and 5 days after administration of TMT (8.0 mg/kg, i.p.). TMT affected the expression of mRNA associated with neurodegeneration (presenilins [PS], tau), synaptic terminals (SNAP 25), mitochondrial function (UCE and LAMP1), stress (GR) and cell signaling related to glial activation (STAT5a) and GSK-3 (β-catenin). Values are mean ± SEM for 4 animals per group. *Significantly different from corresponding saline control, $p<0.05$.

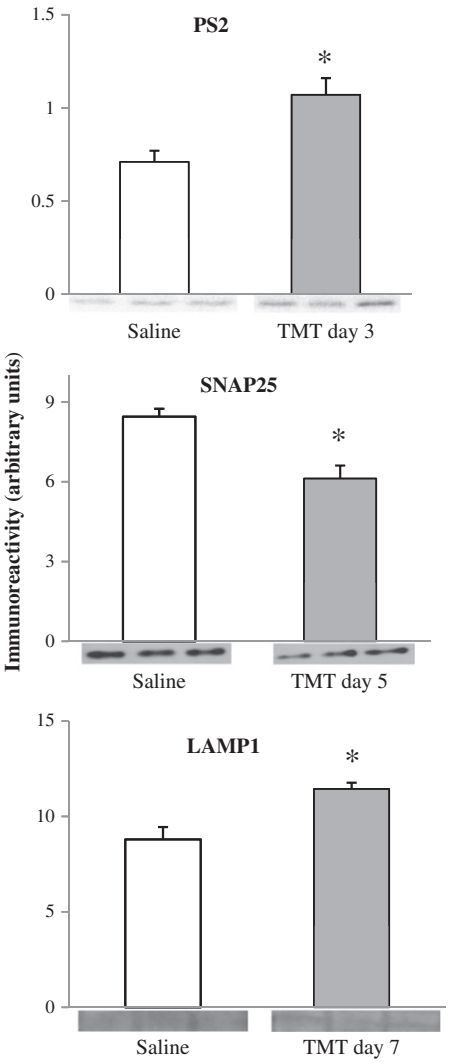

Fig. 5. Changes in hippocampal protein expression by immunoblot analysis at 3–7 days after administration of TMT (8.0 mg/kg, i.p.). Representative immunoblots corresponding to each protein are shown for saline- and TMT-treated rats. Values are mean ± SEM for 3–4 animals per group. *Significantly different from corresponding saline control, $p < 0.05$.

linked to a variety of neurotoxic exposures. When we screened hippocampal samples prepared 3 days after exposure to TMT, genes with expression levels below 0.5 or above 1.5 were few in number and were restricted to small numbers of functional categories. With the exception of neuronal genes, such as synaptophysin, and neurodegeneration and degradation genes, such as presenilin 1 and ubiquitin conjugating enzyme, respectively, no gene clusters stood out as being related to changes that might be expected during the very early stages on TMT-induced neurotoxicity. Moreover, none of the observed changes reached statistical significance. Nevertheless, the microarray data for post-dosing day 3 served to drive highly significant findings in multiple networks and pathways using the Ingenuity Pathway Analysis tool.

Visualization tools now are widely employed to identify and communicate salient findings obtained from high-throughput screens, such as gene microarray analysis (Gehlenborg et al., 2010). Even with the relatively small numbers of genes that appeared to be changed as a function of exposure to TMT at day 3, our intent was not only to find early changes related to neural damage by this compound, but also to visualize and construct pathways which would aid in future exploration of mechanisms underlying neurotoxicity and associated glial responses. An overall goal would be to identify neurotoxicity pathways of broad use in toxicity screening as proposed in the Tox 21 initiative (Hartung, 2009). When we used the IPA tool for this purpose, the summary functions and pathways revealed were, in large measure, those associated with neurological disease, cellular assembly and maintenance, as well as signaling pathways associated with cellular stress, energy metabolism and glial activation. While the decreases in genes associated with cell structure, such as tubulin and MAP1B, could be viewed as down-regulation events associated with changes in cellular morphology in otherwise intact cells, it seems more likely that these changes simply were a reflection of neuropathology already ongoing at this time. Thus, consistent with the silver degeneration staining we observed at post-dosing day 3, alterations in oxidative phosphorylation, induction of GFAP and 14-3-3 scaffolds associated with glial activation, as well as induction of HSP90, all would be expected expression changes associated with neuropathology. Our novel findings of an increase in LAMP1, a lysosomal associated membrane protein also is consistent with this view. LAMP1 can regulate APP, is associated with astrogliosis and autophagy, and is known to play a role in cell death (e.g. see Hashimoto et al., 2010). Finally, the addition of SNAP25 to our prior identification of synapsin I and synaptophysin as synapse-associated entities that decrease following TMT (Brock and O'Callaghan, 1987), also is an observation consistent with neuronal damage or death, either at the level of the neuronal perikarya or as local loses of message/protein in nerve terminals early in the time course of TMT neurotoxicity.

We used the IPA tool to direct our selection of expression candidates for confirmation by q-RT-PCR and immunoblot analyses. The changes seen by q-RT-PCR came from several categories implicated by IPA results, including those associated with neurodegenerative diseases (Tau, presenilins), stress activation (GR), protein processing and degradation (UCE, LAMP1) and cell signaling related to neural damage (STAT5a, B-catenin, SNAP25). While we did not succeed in confirming all q-RT-PCR candidates by immunoblot analysis, perhaps due to the lack of sufficiently sensitive and specific antibodies or examining an inappropriate time point, we did find significant effects on synaptic, neurodegenerative and lysosomal proteins consistent with neural damage. Given that the 3-day post TMT sampling time point coincides with the earliest evidence for hippocampal neuronal damage (Balaban et al., Fig. 1) and microglial activation (McCann et al., 1996), we did not expect to see large changes in gene expression nor the involvement of large numbers of genes or proteins at this early time point. We did anticipate, however, that we might observe expression changes that would implicate mechanisms leading to full-blown neuropathology associated with later time points after administration of TMT. While small in magnitude, changes in the transcripts and proteins that emerged from the IPA, q-RT-PCR and immunoblot analysis included those known to be associated with advanced neurodegenerative disease states. Thus, our findings now suggest that these same transcripts can be involved early, during the induction phase of neuronal damage and gliosis.

Perhaps the most informative data that emerged from the present investigation was the lack of effects of TMT on expression of inflammatory mediators. Neuronal degeneration and subsequent gliosis instigated by TMT were not associated with altered expression of genes in clusters associated with inflammatory responses. Indeed, the IPA-identified network affected the most significantly by TMT showed decreased input through NFκB, a key down-stream effector of inflammatory mediators. Given that microglial and astroglial activation occurs within 3 and 5-days post administration of TMT, respectively (Brock and O'Callaghan, 1987; Little et al., 2002; McCann et al., 1996), evidence for glial-derived or glial-affected proinflammatory cytokine expression should be observed at these time points. When we previously used the TMT model to examine cytokine and chemokine signaling events associated with neural injury, we were surprised to find that extensive hippocampal damage due to this

toxicant was not accompanied by enhanced expression of the key elements of the proinflammatory process (Little et al., 2002). For example, at 1, 2, 3, 5, 7 and 21 days post TMT, we failed to observe increases in TNF-α, IL-1α and IL-1β or IL-6, as assessed by q-RT-PCR and immunoblots or ELISA (Little et al., 2002). Additionally, another prior observation showed that anti-inflammatory pretreatment of rats with corticosterone did not affect TMT-induced neurotoxicity and astrogliosis (O'Callaghan et al., 1991). Together, these previous findings are in concordance with those observed in the present genome-wide survey and data mining by IPA. Nevertheless, a microglial activation response clearly is observed in response to our TMT exposure regimen (McCann et al., 1996) and, in general, this cellular reaction is associated with increased expression of MHC class II molecules, findings often viewed as evidence of inflammation or neuroinflammation (Graeber and Streit, 2010). The activated microglial phenotype most clearly represents a microsensor of underlying neuropathology (Kreutzberg, 1996). Neuropathology can elicit neuroinflammatory responses in association with activation of microglia, but the beneficial or detrimental effects of such responses remain unclear (Graeber and Streit, 2010). In aggregate, our present data are suggestive of another neuropathology phenotype, one in which substantial neuronal loss and ensuing gliosis can occur in the absence of substantial evidence of neuroinflammation.

From the aforementioned it would be tempting to generalize our findings to gene expression changes observed after hippocampal damage associated with other agents or conditions. This would be premature, however, because even for hippocampal damage due to TMT, marked species-specific responses appear to exist. For example, it has been well-established that a variety of neuroinflammatory mediators are expressed in hippocampus after administration of TMT to the mouse (e.g. see Harry et al., 2008). Whereas administration of TMT to the rat results primarily in damage to hippocampal pyramidal neurons, its administration to mice favors damage to dentate granule neurons. Damage to the latter appears to confer a neuroinflammatory phenotype. Thus, a shift of damage to a different neuronal cell type within the hippocampus may engender different gene expression profiles apparently associated with activated microglia (Harry et al., 2008), findings in accordance with the diversity of microglial immunoregulatory markers across and within a given brain region (de Haas et al., 2008; Sriram et al., 2006). Moreover, it also is possible that key inflammatory events underlying TMT neurotoxicity and glial activation were below the level of detection or expressed at an earlier time point (e.g. see Morita et al., 2008) in the present study. Clearly, in contrast to our present data, strong evidence exists for a role of inflammatory processes in a variety of CNS disease states and processes (Block et al., 2007; Gao and Hong, 2008).

In summary, the present findings show that gene-expression changes early in the time course of TMT-induced neurotoxicity encompass categories that include synaptic and neurodegeneration-related networks and protein processing and degradation pathways. The networks and associated genes affected by TMT at post dosing day 3, while related to known damage pathways and events, were not accompanied by neuroinflammatory responses. Combined with the results of our previous studies, we conclude that extensive hippocampal neuronal damage and gliosis can occur in the absence of inflammation and disruption of the blood–brain barrier (Little et al., 2002). Moreover, our results suggest that components of the ubiquitin–proteosome system (UPS) and its down-stream targets known to be associated with neurodegenerative disease (Alves-Rodrigues et al., 1998; Kantamneni et al., 2011), can be very early participants and perhaps instigators of the neurodegenerative process. The effects of the dysregulation of the UPS deserve further evaluation as primary or secondary events leading to neurodegeneration after TMT and in association with a variety of neurodegenerative diseases. Thus, a future focus on the expression domains affected by TMT may serve as the beginning for establishing broadly applicable neurotoxicity pathways that eventually may be used as components of high-throughput toxicity screens (Hartung, 2009).

Conflict of interest statement

Nothing declared.

Acknowledgments

We appreciate the excellent technical assistance provided by Brenda K. Billig and Christopher M. Felton.

References

Alves-Rodrigues A, Gregori L, Figueiredo-Pereira ME. Ubiquitin, cellular inclusions and their role in neurodegeneration. Trends Neurosci 1998;21:516–20.
Andersson H, Luthman J, Olson L. Trimethyltin-induced expression of GABA and vimentin immunoreactivities in astrocytes of the rat brain. Glia 1994;11:378–82.
Balaban CD, O'Callaghan JP, Billingsley ML. Trimethyltin-induced neuronal damage in the rat brain: comparative studies using silver degeneration stains, immunocytochemistry and immunoassay for neuronotypic and gliotypic proteins. Neuroscience 1988;26:337–61.
Banati RB, Myers R, Kreutzberg GW. PK ('peripheral benzodiazepine')-binding sites in the CNS indicate early and discrete brain lesions: microautoradiographic detection of [3H]PK11195 binding to activated microglia. J Neurocytol 1997;26:77–82.
Benjamini Y, Hochberg Y. Controlling the false discovery rate: a practical and powerful approach to multiple testing. J R Stat Soc Ser B 1995;57:289–300.
Block ML, Zecca L, Hong JS. Microglia-mediated neurotoxicity: uncovering molecular mechanisms. Nat Rev Neurosci 2007;8:57–69.
Bo L, Mork S, Kong PA, Nyland H, Pardo CA, Trapp BD. Detection of MHC class II-antigens on macrophages and microglia, but not on astrocytes and endothelia in active multiple sclerosis lesions. J Neuroimmunol 1994;51:135–46.
Brock TO, O'Callaghan JP. Quantitative changes in the synaptic vesicle proteins synapsin I and p38 and the astrocyte-specific protein glial fibrillary acidic protein are associated with chemical-induced injury to the rat central nervous system. J Neurosci 1987;7:931–42.
Cammer W, Tansey FA, Brosnan CF. Gliosis in the spinal cords of rats with experimental allergic encephalomyelitis: immunostaining of carbonic anhydrase and vimentin in reactive astrocytes. Glia 1989;2:223–30.
Chang LW, Tiemeyer TM, Wenger GR, McMillan DE, Reuhl KR. Neuropathology of trimethyltin intoxication. II. Electron microscopic study on the hippocampus. Environ Res 1982;29:445–58.
Chang LW, Dyer RS. A time-course study of trimethyltin induced neuropathology in rats. Neurobehav Toxicol Teratol 1983;5:443–59.
Condorelli DF, Dell'Albani P, Kaczmarek L, Messina L, Spampinato G, Avola R, et al. Glial fibrillary acidic protein messenger RNA and glutamine synthetase activity after nervous system injury. J Neurosci Res 1990;26:251–7.
Cook LL, Heath SM, O'Callaghan JP. Distribution of tin in brain subcellular fractions following the administration of trimethyltin and triethyltin to the rat. Toxicol Appl Pharmacol 1984;73:564–8.
de Haas AH, Boddeke HW, Biber K. Region-specific expression of immunoregulatory proteins on microglia in the healthy CNS. Glia 2008;56:888–94.
de Olmos JS, Beltramino CA, de Olmos de Lorenzo S. Use of an amino-cupric-silver technique for the detection of early and semiacute neuronal degeneration caused by neurotoxicants hypoxia, and physical trauma. Teurotoxicol Teratol 1994;16:545–61.
Eng LF, Ghirnikar RS, Lee YL. Glial fibrillary acidic protein: GFAP-thirty-one years (1969–2000). Neurochem Res 2000;25:1439–51.
Faulkner JR, Herrmann JE, Woo MJ, Tansey KE, Doan NB, Sofroniew MV. Reactive astrocytes protect tissue and preserve function after spinal cord injury. J Neurosci 2004;24:2143–55.
Finsen BR, Jorgensen MB, Diemer NH, Zimmer J. Microglial MHC antigen expression after ischemic and kainic acid lesions of the adult rat hippocampus. Glia 1993;7:41–9.
Gao HM, Hong J. Why neurodegenerative diseases are progressive; uncontrolled inflammation drives disease progression. Trends Immunol 2008;29:357–65.
Gehlenborg N, O'Conoghue SI, Baliga NS, Goesmann A, Hibbs MA, Kitano H, et al. Visualization of omics data for systems biology. Nat Methods 2010;7:S56–8.
Gentleman R, Carey VJ, Bates DM, Bolstad B, Dettling M, Dudoit S, et al. Bioconductor: open software development for computational biology and bioinformatics. Genome Biol 2004;5:R80.
Graeber MB, Streit WJ. Microglia: biology and pathology. Acta Neuropathol 2010;119:89-105.
Guilarte TR, Kuhlmann AC, O'Callaghan JP, Miceli RC. Enhanced expression of peripheral benzodiazepine receptors in trimethyltin-exposed rat brain: a biomarker of neurotoxicity. Neurotoxicology 1995;16:441–50.
Harry GJ, d'Hellencourt CL, McPherson CA, Funk JA, Aoyama M, Wine RN. Tumor necrosis factor p55 and p75 receptors are involved in chemical-induced apoptosis of dentate granule neurons. J Neurochem 2008;106:281–98.
Hartung T. Toxicology for the twenty-first century. Nature 2009;460:208–12.
Hashimoto T, Ogino K, Shin RW, Kitamoto T, Kikuchi T, Shimizu N. Age-dependent increase in lysosome-associated membrane protein 1 and early-onset behavioral

deficits in APPSL transgenic mouse model of Alzheimer's disease. Neurosci Lett 2010;469:273–7.
Hauss-Wegrzyniak B, Dobrzanski P, Stoehr JD, Wenk GL. Chronic neuroinflammation in rats reproduces components of the neurobiology of Alzheimer's disease. Brain Res 1998;780:294–303.
Heiman M, Schaefer A, gong S, Peterson JD, Day M, Ramsey KE, et al. A translational profiling approach for the molecular characterization of CNS cell types. Cell 2008;135:738–48.
Kantamneni S, Wilkinson KA, Henley JM. Ubiquitin regulation of neuronal excitability. Nat Neurosci 2011;14:126–8.
Kreutzberg GW. Microglia: a sensor for pathological events in the. CNS Trends Neurosci 1996;19:312–7.
Kuhlmann AC, Guilarte TR. The peripheral benzodiazepine receptor is a sensitive indicator of domoic acid neurotoxicity. Brain Res 1997;751:281–8.
Kuhlmann AC, Guilarte TR. Regional and temporal expression of the peripheral benzodiazepine receptor in MPTP neurotoxicity. Toxicol Sci 1999;48:107–16.
Laemmli UK. Cleavage of structural proteins during the assembly of the head of bacteriophage T4. Nature 1970;227:680–5.
Little AR, Benkovic SA, Miller DB, O'Callaghan JP. Chemically induced neuronal damage and gliosis: enhanced expression of the proinflammatory chemokine, monocyte chemoattractant protein (MCP)-1, without a corresponding increase in proinflammatory cytokines. Neuroscience 2002;115:307–20.
McCann MJ, O'Callaghan JP, Martin PM, Bertram T, Streit WJ. Differential activation of microglia and astrocytes following trimethyl tin-induced neurodegeneration. Neuroscience 1996;72:273–81.
McTigue DM, Tani M, Krivacic K, Chernosky A, Kelner GS, Maciejewski D, et al. Selective chemokine mRNA accumulation in the rat spinal cord after contusion injury. J Neurosci Res 1998;53:368–76.
Mikucki SA, Oblinger MM. Vimentin mRNA expression increases after corticospinal axotomy in the adult hamster. Metab Brain Dis 1991;6:33–49.
Morita M, Imai H, Liu Y, Xu X, Sadamatsu M, Nakagami R, et al. FK506-protective effects against trimethyltin neurotoxicity in rats: hippocampal expression analyses reveal the involvement of periarterial osteopontin. Neuroscience 2008;153:1135–45.
Norenberg MD. The reactive astrocyte. In: Aschner M, Costa L, editors. The role of glia in neurotoxicity. 2nd ed. Boca Raton: CRC Press; 2005. p. 73–92.
O'Callaghan JP. Neurotypic and gliotypic proteins as biochemical markers of neurotoxicity. Neurotoxicol Teratol 1988;10:445–52.
O'Callaghan JP. Quantitative features of reactive gliosis following toxicant-induced damage of the CNS. Ann NY Acad Sci 1993;679:195–210.
O'Callaghan JP, Brinton RE, McEwen BS. Glucocorticoids regulate the synthesis of glial fibrillary acidic protein in intact and adrenalectomized rats but do not affect its expression following brain injury. J Neurochem 1991;57:860–9.
O'Callaghan JP, Jensen KF, Miller DB. Quantitative aspects of drug and toxicant-induced astrogliosis. Neurochemistry 1995;26:115–24.
O'Callaghan JP, Miller DB. Quantification of reactive gliosis as an approach to neurotoxicity assessment. NIDA Res Monogr Ser 1993;136:188–212.
O'Callaghan JP, Imai H, Miller DB, Minter A. Quantitative immunoblots of proteins resolved from brain homogenates: underestimation of specific protein concentration and of treatment effects. Anal Biochem 1999;274:18–26.
O'Callaghan JP, Sriram K. GFAP and other glial proteins as biomarkers of neurotoxicity. Expert Opin Drug Saf 2005;4:433–42.
Seo J, Gordish-Dressman H, Hoffman EP. An interactive power analysis tool for microarray hypothesis testing and generation. Bioinformatics 2006;22:808–14.
Shaw JA, Perry VH, Mellanby J. MHC class II expression by microglia in tetanus toxin-induced experimental epilepsy in the rat. Neuropathol Appl Neurobiol 1994;20:392–8.
Smith PK, Krohn RI, Hermanson GT, Mallia AK, Gartner FH, Provenzano MD, et al. Measurement of protein using bicinchoninic acid. Anal Biochem 1985;150:76–85.
Sofroniew MV. Reactive astrocytes in neural repair and protection. Neuroscientist 2005;11:400–7.
Sofroniew MV. Molecular dissection of reactive astrogliosis and glial scar formation. Trends Neurosci 2009;32:638–47.
Sriram K, Matheson JM, Benkovic SA, Miller DB, Luster MI, O'Callaghan JP. Microglial activation and MPTP-induced neurotoxicity: region-specific role for TNF-α. FASEB J 2006;20:670–82.
Stringer JL. Repeated seizures increase GFAP and vimentin in the hippocampus. Brain Res 1996;717:147–53.
Streit WJ. The role of microglia in neurotoxicity. In: Aschner M, Costa L, editors. The role of glia in neurotoxicity. 2nd Edition. Boca Raton: CRC Press; 2005. p. 29–40.
Tobin H, Staehelin T, Gordon J. Electrophoretic transfer of proteins from polyacrylamide gels to nitrocellulose sheets: procedure and some applications. Proc Natl Acad Sci U S A 1979;76:4350–4.
Vogt BA. Vogt's method for nerve cell products. In: Luna LG, editor. New York: McGraw-Hill Company; 1968. p. 206.
Whittington DL, Woodruff ML, Baisden RH. The time-course of trimethyltin-induced fiber and terminal degeneration in hippocampus. Neurotoxicol Teratol 1989;11:21–33.
Xu J, Ling EA. Upregulation and induction of surface antigens with special reference to MHC class II expression in microglia in postnatal rat brain following intravenous or intraperitoneal injections of lipopolysaccharide. J Anat 1994;184(Pt 2):285–96.